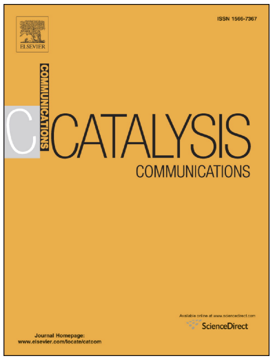

Heterogeneous simplified Maruoka phase-transfer catalyst tethered on poly(styrene-co-acrylamide) microsphere: Structure-activity relationship in enantioselective α-alkylation

Dandan Feng, Jingwei Wan, Fei Teng, Xuebing Ma

PII: S1566-7367(17)30233-9
DOI: doi: 10.1016/j.catcom.2017.06.002
Reference: CATCOM 5068

To appear in: *Catalysis Communications*

Received date: 1 April 2017
Revised date: 4 June 2017
Accepted date: 6 June 2017

Please cite this article as: Dandan Feng, Jingwei Wan, Fei Teng, Xuebing Ma , Heterogeneous simplified Maruoka phase-transfer catalyst tethered on poly(styrene-co-acrylamide) microsphere: Structure-activity relationship in enantioselective α-alkylation. The address for the corresponding author was captured as affiliation for all authors. Please check if appropriate. Catcom(2017), doi: 10.1016/j.catcom.2017.06.002

Heterogeneous simplified Maruoka phase-transfer catalyst tethered on poly(styrene-*co*-acrylamide) microsphere: structure -activity relationship in enantioselective *α*-alkylation

Dandan Feng,[a] Jingwei Wan,[b] Fei Teng,[a] and Xuebing Ma*[a]

[a] *Key Laboratory of Applied Chemistry of Chongqing Municipality, College of Chemistry and Chemical Engineering, Southwest University, Chongqing, 400715, P. R. China*; [b] *Railway Police College, Henan, 450053, P. R. China*

* Corresponding author. Tel.: +86-23-68252360;
fax: +86-23-68254000.
E-mail addresses: zcj123@swu.edu.cn (X.B. Ma),

Abstract

The covalent immobilization of valuable simplified Maruoka catalyst onto poly(styrene-*co*-acrylamide)microsphere at different locations was developed for the first time through the copolymerization of Maruoka catalyst-functionalized styrene with styrene and acrylamide cross-linked by EGDMA. It was found the morphology, porous feature of microsphere and the anchor location of Maruoka catalyst were mainly responsible for the catalytic performance in heterogeneous *α*- alkylation. The catalyst poly[St-*co*-AA-*co*-(*R*)-11] with a rigid framework, where homogeneous (*R*)-11 was anchored at the 6, 6'-positions of binaphthyl skeleton, possessed the relatively larger surface area (33.5 m^2 g^{-1}) and pore volume (1.27 cc g^{-1}) and displayed high yields (81–96%) and excellent enantioselectivities (96–97 %ee) in enantioselective *α*-alkylation.

Keywords: Simplified Maruoka catalyst; Heterogeneous catalysis; Poly(styrene-*co*-acrylamide) microsphere; Structure-activity relationship; Asymmetric *α*-alkylation

1. Introduction

Asymmetric phase-transfer catalysis (PTC) by means of a chiral quaternary ammonium salt has been recognized as one of the most practical methodologies in the enantioselective synthesis of highly valuable and optically active natural and non-natural organic compounds through carbon-carbon or carbon-heteroatom bond-forming reactions under mild biphasic conditions [1, 2]. Owing to the importance of PTC in enantioselective synthesis, the various categories of chiral phase-transfer catalysts (PTCs), especially well-known representatives such as cinchona alkaloid and binaphthyl-derived PTCs, had been well developed for organic synthesis in both industry and academia [3]. Up to now these privileged chiral PTCs were efficiently utilized for a wide variety of asymmetric transformations such as α-alkylation [4–7], conjugate addition [8, 9], Mannich reaction [10], Michael addition [11], aldol reaction [12] and cascade reaction [13]. From the viewpoint of green sustainable chemistry, it was well known that homogeneous catalyst could be generally heterogenized onto solid supports (e.g., inorganic material or polymer) to achieve the sustainability *via* (i) covalent bonding, (ii) adsorption or ion-pair formation, (iii) encapsulation and (iv) entrapment [14, 15]. To achieve the reusability of homogeneous PTCs, several reports focused on polymeric [16–20] and inorganic material [21, 22]-supported cinchona alkaloid-derived PTCs had been investigated in detail. However, there were the limited reports on the recovery and reusability of versatile and extraordinarily expensive Maruoka PTCs owing to the difficult functionalization of binaphthyl skeleton [23–26]. Early in 2004, K. Maruoka developed a fluorous chiral binaphthyl-modified spiro-type quaternary ammonium salt attached with the 4, 4´, 6, 6´-*tetra*-substituted $C_8F_{17}CH_2CH_2SiMe_2$ groups, which could be recovered though liquid/liquid biphasic separation by using fluorous perfluorohexane (FC-72) as an extractant in the asymmetric synthesis of α-amino acids [27]. In 2008, S. Itsuno et al. immobilized Maruoka PTCs onto sulfonated polymer through the ionic bond interaction between quarternary ammonium cation and sulfonate anion [28].

Despite their excellent catalytic performances of reusable Maruoka PTCs, these two strategies actually still had the drawbacks of the laborious fluorous liquid/liquid separation and less stability of PTCs against leaching of cationic species in catalytic medium, respectively. Generally, the covalent immobilization of homogeneous chiral catalyst onto solid support *via* covalent bond is the most often employed method to heterogenize stereoselective catalyst in view of enhanced stability in reuse [29–32]. To our knowledge, the covalent linkage of well-known Maruoka PTCs onto whatever inorganic or polymeric materials was never reported up to now, possibly owing to the difficult functionalization of the inert skeleton of Maruoka PTCs. In this work, we endeavoured to introduce two anchorage points of carbon-carbon double bond in styrene moiety into the skeleton of simplified Maruoka catalyst through two routes, in which one of the rigid binaphthyl moieties in Maruoka PTCs was replaced by flexible straight-chain alkyl groups to furnish new simplified Maruoka PTCs [33]. This is the first example of the immobilization of simplified Maruoka PTCs into polystyrene microspheres through the covalent immobilization (**Scheme 1**).

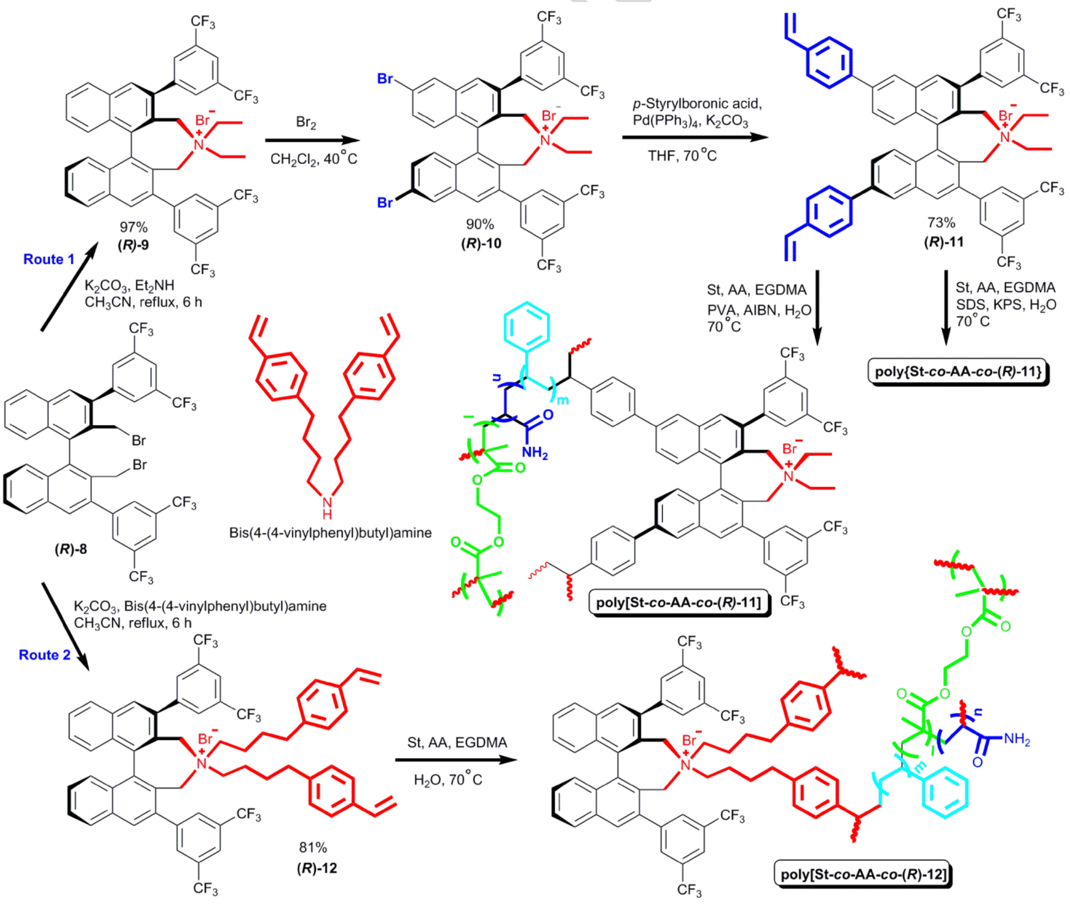

Scheme 1 The routes to the covalent immobilization of simplified Maruoka PTCs onto polystyrene microspheres

2. Experimental

2.1. Materials

Styrene (St) was pre-treated with aqueous NaOH solution (10 %) and distilled under reduced pressure to remove polymerization inhibitor completely. The initiator azobisisobutyronitrile (AIBN) was further purified by ethanol recrystallization. The intermediates (*R*)-8 [33, 34], (*R*)-11, (*R*)-12 and bis(4-(4-vinylphenyl)butyl)amine were synthesized according to the procedure shown in ESI† and their structures were evidenced by ^{1}H and ^{13}C NMR.

2.2. Preparation of microsphere-supported Maruoka catalysts

Suspension polymerization: To the well-stirred solution of acrylamide (AA) (53.3 mg, 0.75 mmol) and poly(vinyl alcohol) (PVA, 20.0 mg, 0.4 wt%) in DI water (5.0 mL) was added a mixture of (*R*)-11 (53.0 mg, 0.05 mmol), styrene (St, 312.4 mg, 3.0 mmol), initiator AIBN (21.3 mg, 0.13 mmol) and ethyleneglycol dimethacrylate (EGDMA, 75.3 mg, 0.38 mmol) by syringe under Ar atmosphere and well stirred for 2 h. Then the resulting emulsion was stirred at 70 °C for another 24 h and diluted with ethanol (15 mL). The yellow granules were filtered, washed with ethanol (5 mL × 3), toluene (5 mL × 3) and dried in *vacuo* at 60 °C to afford supported simplified Maruoka catalyst poly[St-*co*-AA-*co*-(*R*)-11] (318.5 mg).

According to the above-mentioned procedure, the other supported simplified Maruoka catalysts were also prepared and designated as a control poly[St-*co*-AA] (232.3 mg) in the absence of (*R*)-11, poly[St-*co*-AA-*co*-(*R*)-11]′ (233.9 mg) and poly[St-*co*-AA-*co*-(*R*)-11]″ (230.5 mg) upon the added amount of PVA set to 1.0 wt% and 4.0 wt%, poly[St-*co*-(*R*)-11] (281.5 mg) in the absence of AA, poly[St-*co*-(AA)-*co*-(*R*)-11] (275.9 mg) upon the decreased St (234.3 mg, 2.3 mmol) and increased AA (106.6 mg, 1.5 mmol), and poly[St-*co*-AA-*co*-(*R*)-12] (261.8 mg) instead of (*R*)-11 with (*R*)-12.

Emulsion polymerization: Instead of initiator AIBN and emulsifier PVA with potassium persulfate (KPS) and sodium dodecyl sulfate (SDS), poly{St-*co*-AA-*co*-(*R*)-11} (210.4 mg) was prepared through emulsion polymerization according to the same procedure as poly[St-*co*-AA-*co*-(*R*)-11].

2.3. General enantioselective α-alkylation reaction

To a mixture of poly[St-*co*-AA-*co*-(*R*)-11] (40.0 mg, 5.6 mol%), *N*-(diphenylmethylene)glycine *tert*-butyl ester (28.5 mg, 0.1 mmol), aqueous KOH solution (50wt%, 0.45 mL,8.0mmol) and toluene (1.0 mL) was added various substituted benzyl bromides (0.5 mmol), cooled to -20 °C and vigorously stirred for 72 h. the resulting reaction mixture was diluted with DI water (5 mL) and ether (5 mL). The catalyst poly[St-*co*-AA-*co*-(R)-11] was recovered by filtration. The filtrate was extracted with ether (5 mL × 2). The combined organic phases were dried over anhydrous Na_2SO_4 and concentrated under reduced pressure to afford the crude *α*-alkylation product, which was purified by gradient column chromatography on alumina gel using petroleum ether/ethyl acetate (*v*/*v* = 60/1 → 40/1) as eluents to afford pure *α*-alkylation products.

3. Results and discussion

3.1. Immobilization and loading capacity of PTCs

The conformationally rigid spiro-type structure of binaphthyl-modified chiral PTCs imposes a limitation on the co-valent immobilization of Maruoka PTCs owing to the lack of active reaction site. In this communication, we endeavoured to introduce styrene moieties as anchorage points at the different locations in the framework of simplified Maruoka PTCs through two routes to achieve the covalent immobilization of Maruoka PTCs (**Scheme 1**). The first route was the bromi-nation of (*R*)-9 and then Suzuki coupling of *p*-styrylboronic acid with (*R*)-10 to afford (*R*)-11 with two styrene-attached moieties at the 6, 6'-positions of binaphthyl skeleton. The second route provided a direct method for the simultaneous generation of quaternary ammonium catalytic site and styrene anchorage points by the nucleophilic substitution of (*R*) -8 with bis(4-(4-vinylphenyl)butyl)amine to afford (*R*)-12. Subsequently, in PVA-emulsified aqueous system, the as-synthe-sized (*R*)-11 and (*R*)-12 were covalently immobilized into the polymeric backbone of poly[St-*co*-AA-*co*-(*R*)-11] and poly[St-*co*-AA-*co*-(*R*)-12] by the suspension polymerization of (*R*)-11 and (*R*)-12 with AA and St monomers cross-linked by EGDMA, respectively. The distinct difference in the structure between poly[St-*co*-AA-*co*-(*R*)-11] and poly[St-*co*-AA-*co*-(*R*)-12] was the different distance of polystyrene backbone to the quaternary ammonium catalytic site. The quaternary ammonium catalytic sites in poly[St-*co*-AA-*co*-(*R*)-11] were located in the rooms far away from the polymer chain and remained the original structure feature of simplified Maruoka PTCs to a great extent owing to the rigid styrene anchorage points. In the other hand, the quaternary ammonium catalytic sites in poly[St-*co*-AA-*co*-(*R*)-12] were linked to polymeric primary chain though the flexible alkyl chains, which resulted in the less rigidity of poly[St-*co*-AA-*co*-(*R*)-12] than that of poly[St-*co*-AA-*co*-(*R*)-11]. From the SEM images (Fig.1), both poly[St-*co*-AA-*co*-(*R*)-11] and poly[St-*co*-AA-*co*-(*R*)-12] showed the similar microsphere morphology in the range of 40–200 um. Based on the contents of nitrogen determined by elemental analysis, poly[St-*co*-AA-*co*-(*R*)-11] and poly[St-*co*-AA-*co*-(*R*)-12] also possessed the same loading capacity of (*R*)-11 and (*R*)-12 (0.14 mmol g^{-1}). However, the utilization of (*R*)-12 (73%) in the preparation process was lower than that of (*R*)-11 (89%), possibly due to the steric hindrance of binaphthyl moieties near to styrene anchorage points in poly[St-*co*-AA-*co*-(*R*)-12] .

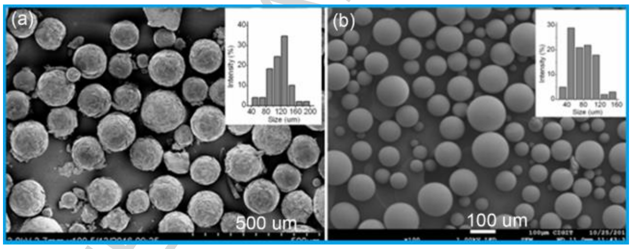

Fig. 1 The SEM images of poly[St-*co*-AA-*co*-(*R*)-11] (c) and poly[St-*co*-AA-*co*-(*R*)-12].

The covalent attachment of simplified Maruoka catalyst (*R*)-11 to the microsphere poly[St-*co*-AA-*co*-(*R*)-11] *via* the copolymerization of C=C double bonds was clearly corroborated by FT-IR spectroscopy (**Fig. S2**). The loading capacities of (*R*)-11 in various polymer-supported PTCs were calculated according to the contents of nitrogen obtained from elemental analysis, and the utilization of (*R*)-11 was evaluated by the mass ratios of loaded (*R*)-11 to added (*R*)-11 (**Table 1**). First of all, the control polymer poly[St-*co*-AA] possessed the low loading capacity of AA (0.16 mmol g^{-1}) with only 5% utilization of added AA based on 0.23% of nitrogen. Secondly, upon increasing the added amount of emulsifier PVA from 0.4 wt% to 4.0 wt%, the loading capacities of (*R*)-11 in poly[St-*co*-AA-*co*-(*R*)-11]′ (0.19 mmol g^{-1}) and poly[St-*co*-AA-*co*-(*R*)-11]″ (0.20 mmol g^{-1}) with the good utilizations of (*R*)-11 (89–92%) were slightly improved owing to the better emulsified effect. Thirdly, the added amount of AA, whatever decreased or increased, had no significant influence on the loading capacity of (*R*)-11 with the good utilizations of (*R*)-11 (83–90%). It was noticeable that the as-synthesized poly{St-*co*-AA-*co*-(*R*)-11} *via* emulsion polymerization exhibited the slightly higher loading capacity (0.18 mmol g^{-1}) and lower utilization (76%) of (*R*)-11 than poly[St-*co*-AA-*co*-(*R*)-11] *via* suspension polymerization.

Table 1 The loading capacities and efficient utilizations of (*R*)-11 and (*R*)-12 determined by elemental analysis

Entry	Sample	N content (%) [a]	Loading capacity (mmol g^{-1}) [b]	Utilization of Cat. (%) [c]
1	poly[St-*co*-AA]	0.23	0.16 [c]	5 [c]
2	poly[St-*co*-AA-*co*-(*R*)-12]	0.42	0.14	73
3	poly[St-*co*-AA-*co*-(*R*)-11]	0.43	0.14	89
4	poly[St-*co*-AA-*co*-(*R*)-11]′	0.49	0.19	89
5	poly[St-*co*-AA-*co*-(*R*)-11]′′	0.51	0.20	92
6	poly[St-*co*-(*R*)-11]	0.22	0.16	90
7	poly[St-*co*-(AA)-*co*-(R)-11]	0.41	0.15	83
8	poly{St-*co*-AA-*co*-(*R*)-11}	0.48	0.18	76

[a] Determined by elemental analysis. [b] Based on the content of nitrogen. [c] The mass ratio of loaded PTCs to added PTCs.

3.2. Surface morphology of supported simplified Maruoka PTCs

The preparation conditions played an important role in surface morphology of supported Maruoka PTCs (**Fig. S7**). The catalyst poly[St-*co*-AA-*co*-(*R*)-11] presented the spherical microsphere in the range of 40–200 um centered at 120–140 um. Upon increasing the added PVA from 0.4 wt% to 1.0 wt% and 4.0 wt%, poly[St-*co*-AA-*co*-(*R*) -11]′ and poly[St-*co*-AA-*co*-(*R*)-11]′′ became smaller, especially for poly[St-*co*-AA-*co*-(*R*)-11]′′ with the 3–21 um diameters centered at 4–8 um owing to the improved emulsification at high PVA concentration. Furthermore, poly[St-*co*-(*R*)-11] (60–110 um) containing no AA possessed the relatively smaller diameter than the poly[St-*co*-AA-*co*-(*R*)-11] and poly[St-*co*-(AA)-*co*-(*R*)-11] with increased AA exhibited a slight variation in the diameter (80–160 um), which implied that AA monomer had an influence in the diameter of supported Maruoka PTCs to a certain degree. By contrast, poly{St-*co*-AA-*co*-(*R*)-11} by emulsion polymerization showed the submicron size and irregular shape (<2 um) accumulated from mutually adherent nanoparticles (<50 nm) (**Fig. S5**).

3.3. Porous structure feature

The porous structures and surface areas of polymer-supported simplified Maruoka PTCs were illustrated by N_2 adsorption–desorption isotherms obtained at 77 K (**Fig. S3**), and their BET-specific surface areas, average pore diameters and pore volumes were listed in **Table S2**. The microsphere poly[St-*co*-AA-*co*-(*R*)-11] possessed the largest surface area (33.5 m^2 g^{-1}), average pore diameter (75.8 nm) and pore volumes (1.27 cc g^{-1}), which favoured the mass transfer of reactants and products into and out from the heterogeneous matrix. When the added PVA increased from 0.4 wt% to 1.0 wt% and 4.0 wt% respectively, poly[St-*co*-AA-*co*-(*R*)-11]′ and poly [St-*co*-AA-*co*-(*R*)-11]″ exhibited the decreased surface areas, pore diameters and pore volumes. Whatever no added AA or increased AA monomer, both poly[St-*co*-(*R*)-11] and poly[St-*co*-(AA)-*co*-(*R*)-11] gave the disappointing average pore diameters and pore volumes. It was concluded that poly[St-*co*-AA-*co*-(*R*)-11] with the molar ratio of St/AA = 4/1 could construct the optimal porous structure for polymer-supported Maruoka PTCs. Furthermore, the poly{St-*co*-AA-*co*-(*R*)-11} with the poor surface area (7.6 m^2 g^{-1}), average pore diameter (4.6 nm) and pore volume (0.017 cc g^{-1}) indicated that emulsion polymerization could not construct a fine porous structure suitable for heterogeneous catalysis. Moreover, poly[St-*co*-AA-*co*-(*R*)-12] with the styrene anchorage point near to the quaternary ammonium bromide catalytic site displayed the poor porous feature.

The pore size distributions (PSDs) of various Maruoka PTCs possessed the similar micro/mesoporous cavities centered at 0.8, 1.3, 1.9, 2.7 and 5.8 nm (**Fig. S4**). Under the improved emulsion system, some characteristic pores disappeared and the irregular PSDs were observed for poly[St-*co*-AA-*co*-(*R*) -11]′ and poly[St-co-AA-co-(*R*)-11]″, accompanied by the low adsorption Dv(r) (0–20 × 10^{-4} cc $Å^{-1}$ g^{-1}). Especially, it was worthwhile to note that poly[St-*co*-AA-*co*-(*R*)-11] afforded the highest nitrogen adsorption Dv(r) (0–10 × 10^{-3} cc $Å^{-1}$ g^{-1}) among the as-prepared supported PTCs. Therefore, It was concluded that the suspension polymerization in 0.4 wt% PVA-emulsified aqueous solution with the molar ratio of (*R*)-11/AA/EGDMA/St = 1/7.5/15/60 could construct the microsphere poly[St-*co*-AA-*co*-(*R*)-11] with fine porous structure and large surface area.

3.4. *Structure-activity relationship in asymmetric α-alkylation*

In the previous literatures, seldom was reported on the structure/activity relationship between the surface morphology, porous feature of polymer-supported catalysts and catalytic performance [35]. In this work, it was found that the structures such as surface morphology, porous feature and anchorage location of Maruoka PTCs played an important role in the catalytic performance of polymer-supported Maruoka PTCs in enantioselective *α*-alkylation.

Table 2 The enantioselective *α*-alkylation of *N*-(diphenylmethylene)glycine *tert*-butyl ester catalyzed by various supported Maruoka PTCs [a]

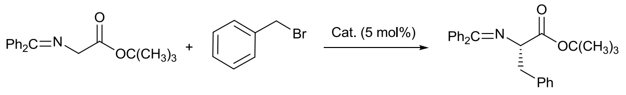

Entry	Cat.	Yield (%) [b]	(%ee) [c]
1	poly[St-*co*-AA-*co*-(*R*)-11]	67	96
2	poly[St-*co*-AA-*co*-(*R*)-11]′	60	94
3	poly[St-*co*-AA-*co*-(*R*)-11]″	52	89
4	poly[St-*co*-(*R*)-11]	51	94
5	poly[St-*co*-(AA)-*co*-(R)-11]	56	96
6	poly{St-*co*-AA-*co*-(*R*)-11}	26	84
7	poly[St-*co*-AA-*co*-(*R*)-12]	58	94

[a] Reaction conditions: Cat. (5.0 mol%), BnBr (85.5 mg, 0.5 mmol), *N*-(diphenylmethylene)glycine *tert*-butyl ester (29.5 mg, 0.1 mmol), KOH (50 wt%, 0.15 mL, 2.7 mmol), toluene (1.0 mL), 0 °C, 48 h. [b] Isolated yield. [c] Determined by HPLC on Phenomenex Lux 5u Amylose-2 chiral column.

Under the same catalytic reactions at 0 °C for 48 h, the catalytic performances of supported Maruoka PTCs were listed in **Table 2**. It was found that the surface morphology, porous feature and anchorage location of Maruoka PTCs were responsible for the yield and enantioselectivity in enantioselective *α*-alkylation. First of all, due to the fine porous feature with the large surface area (33.5 m^2 g^{-1}), average pore diameter (75.8 nm) and pore volume (1.27 cc g^{-1}), poly[St-*co*-AA-*co*-(*R*)-11] *via* suspension polymerization exhibited the higher catalytic performances (67%, 96 %ee) than poly{St-*co*-AA-*co*-(*R*)-11} *via* emulsion polymerization (26%, 84 %ee), even though poly{St-*co*-AA-*co*-(*R*)-11} possessed the smaller submicron size and higher loading capacity of (*R*)-11. Secondly, under the improved emulsification at 4.0 wt% PVA concentration, poly[St-*co*-AA-*co*-(*R*)-11]″ with the smaller diameter (3–21 um) showed the sharply reduced surface area (16.1 m^2 g^{-1}), average pore diameter (11.9 nm) and pore volume (9.6 × 10^{-2} cc g^{-1}), which ultimately resulted in the disappointed catalytic performances (52%, 89 %ee). When the used amounts of AA were further screened, both poly[St-*co*-(*R*)-11] and poly[St-*co*-(AA)-*co*-(*R*)-11] afforded *α*-alkylation products in the inferior yields to poly[St-*co*-AA-*co*-(*R*)-11] due to the reduced surface area, average pore diameter and pore volume. Especially, the anchorage location of homogeneous Maruoka PTCs had a great influence on catalytic performances including activity and steroselectivity. It was found that poly[St-*co*-AA-*co*-(*R*)-12] with styrene anchorage points through flexible alkyl chain connected to quarternary ammonium catalytic site exhibited the lower yield (58%) and slightly poorer enantioselectivity (94 %ee) than poly[St-*co*-AA-*co*-(*R*)-11]. The low surface area and poor porous feature were responsible for the lower yield, whereas the poorer enantioselectivity was attributed to the rigidity of polymeric framework. For poly[St-*co*-AA-*co*-(*R*)-11], (*R*)-11 was covalently bonded to the polymeric chain through phenyl with *π*-*π* conjugation effect. It was easier for poly[St-*co*-AA-*co*-(*R*)-11] with a good rigidity to remain the original conformation of homogeneous Maruoka PTCs. However, (*R*)-12 was covalently bonded to the polymeric chain through the flexible alkyl group, which would result in the subtle change in the conformation of quaternary ammonium catalytic site. In the catalytic process, this subtle change in conformation affected the interaction of ammonium catalytic site with the incoming substrates and the decreasing in enantioselectivity was obtained.

It was worthwhile to note that the really catalyst's porous structure in α-alkylation was more complex than the measured values owing to the swelling of polymer backbone in reaction medium. Owing to the complete insolubility in various polar and non-polar solvents, the different chiral subtle microenvironments in polymer-supported Maruoka PTCs are difficult to be clarified by CD spectrometry. As an alternative to elucidate the different subtle microenvironments, the solid state ^{13}C MAS NMR spectra of poly{St-*co*-AA-*co*-(*R*)-11} with the inferior enantioselectivity (84 %ee) displayed no peaks of aromatic ring at 166.5 ppm and 136.4 ppm (**Fig. S8**), which implied that the binaphthyl moiety in poly{St-*co*-AA-*co*-(*R*)-11} possessed the different subtle microenvironments. Furthermore, under the improved emulsification at 4.0

wt% PVA, the obtained poly[St-*co*-AA-*co*-(*R*)-11]″ showed the same absorption peaks of binaphthyl moiety as poly[St-*co*-AA-*co*-(*R*)-11] in the 100–250 ppm range and different absorption peaks of alkyl carbon in the 10–80 ppm range, which illustrated that the emulsification played an important role on the subtle microenvironments of alkyl chain near to the catalytic site of quaternary ammonium. On the whole, the subtle microenvironments under different polymerizations were the major sources of catalytic performances including activity and enantioselectivity.

3.5. Heterogeneous enantioselective α-alkylation

After the *α*-alkylation catalytic conditions such as temperature, used amount of poly[St-*co*- AA-*co*-(*R*)-11] and base were further optimized, the heterogeneous *α*-alkylation of *N*-(diphenylmethylene)glycine *tert*-butyl ester with benzyl bromide, catalyzed by 5.6 mol% of poly[St-*co*-AA-*co*-(*R*)-11] at -20 °C in toluene (1.0 mL) for 72 h, gave the product in high yield (96%) with excellent enanotioselectivity (97 %ee) (**Table 3**, **Entry 1**). With the optimized conditions at hand, the effect of styrene anchorage location on *α*-alkylation of *N*-(diphenylmethylene)glycine *tert*-butyl ester with *o*, *m*, *p*-methylbenzyl bromides was further investigated in detail. Just as above- mentioned experimental phenomena (**Table 2**, **Entry 7**), the microsphere poly[St-*co*-AA-*co*-(*R*)-11] displayed the superior yields and enantioselectivities (81–96 %, 96 –97 %ee) to poly[St-*co*-AA-*co*-(*R*)-12] (78–88%, 88–95 %ee). Encouraged by the remarkable catalytic results under the optimal catalytic conditions, the substrate scope of electrophiles was extended to various *o*, *m*, *p*-CH_3, F, CF_3 and NO_2-substituted benzyl bromides, allyl bromides and propargyl bromide. It was found that the various benzyl bromides, both with electron-withdrawing (–F, –CF_3 and –NO_2) and electron-donating (–CH_3) groups, could produce the corresponding *α*-alkylation products with good to excellent yields (76–96%) and enantioselectivities (88–97 %ee). In particular, compared with benzyl bromides bearing the *m*, *p*-CF_3, F, CH_3 and NO_2 substituents, the electrophiles bearing *o*-CF_3, F, CH_3 and NO_2 substituents exhibited the poor yields owing to the steric hindrance resulted from the confined interaction between the benzyl bromides with *o*-CF_3, F, CH_3 and NO_2 substituents and glycine *tert*-butyl ester in heterogeneous *α*-alkylation (**Entries 2, 5, 8, 11, Table 3**). Moreover, unlike other heterogeneous PTCs [25], the allyl and propargyl bromides could afford the corresponding *α*-alkylation products in good yields (77–91%) with satisfactory enantioselectivities (93–97 %ee) (**Entries 14–16, Table 3**). However, due to the mass transfer limitation of reactants and embedding active catalytic sites in heterogeneous phase, poly[St-*co*-AA-*co*-(*R*)-11] displayed the lower catalytic activities and required significantly prolonged reaction times to achieve the similar yields as homogeneous (*R*)-11.

Table 3 Enantioselective phase-transfer *α*-alkylation of *N*-(diphenylmethylene)glycine *tert*-butyl ester using different electrophiles[a]

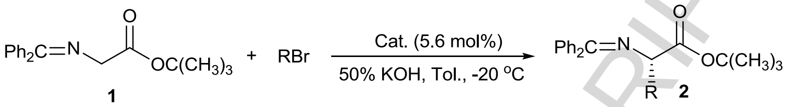

Entry	RBr	Time (h)	Yield (%) ^{b}	(%ee) ^{c}
1	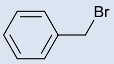	72	96	97
		4 ^{e}	96	97
		72 ^{f}	86	93
		10 ^{g}	95	96
2	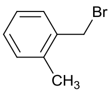	72	81	96
		7 ^{e}	96	97
		72 ^{f}	78	95
		10 ^{g}	95	98
3	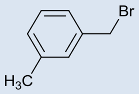	72	93	97
		3 ^{e}	96	97
		72 ^{f}	84	88
		10 ^{g}	94	96
4	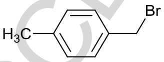	72	93	96
		3 ^{e}	96	97
		72 ^{f}	88	90
		10 ^{g}	93	96
5	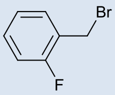	72	85	96
		10 ^{e}	96	97
6	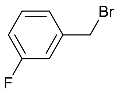	72	90	97
		3 ^{e}	96	97
7	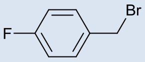	72	96	97
		7 ^{e}	96	97

8	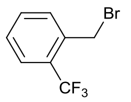	72 3[e]	76 96	97 97
9	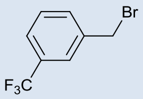	72 8[e]	90 96	96[d] 96[d]
10	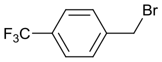	72 3[e]	76 96	96 96
11	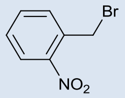	72 12[e]	89 95	89 91
12	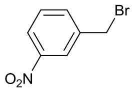	60 3[e]	93 95	88 95
13	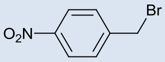	72 3[e]	90 95	89 96
14	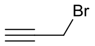	72 3[e]	77 92	97 97
15	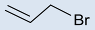	72 3[e]	91 93	95 96
16	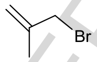	72 3[e]	82 92	93 90

---

[a] Reaction conditions: poly[St-*co*-AA-*co*-(*R*)-11] (40 mg, 5.6 mol%), benzyl bromide derivatives (0.5 mmol), *N*-(diphenylmethylene) glycine *tert*-butyl ester (28.5 mg, 0.1 mmol), KOH aq. (50 wt%, 0.45 mL, 8.0 mmol), toluene (1.0 mL), -20 °C. [b] Isolated yield. [c] Determined by chiral HPLC with Phenomenex Lux 5u Amylose-2 chiral column. [d] Daicel Chiralpak OD-H column. [e] Homogeneous (*R*)-11. [f] poly[St-*co*-AA-*co*-(*R*)-12]. [g] Homogeneous (*R*)-12.

3.6. Reusability

After the completion of *α*-alkylation, the microsphere poly[St-*co*-AA-*co*-(*R*)-11] could be recovered by filtration and reused directly for the next run without further treatment. The recovered poly[St-*co*-AA-*co*-(*R*)-11] in the third reuse exhibited the significantly enhanced catalytic activity and afforded *α*-alkylation product in high yield (96%) within the shortened 48 h. Unfortunately, the reduced enantioselectivities from 97 %ee to 91 %ee were observed in the fifth run. In order to clarify the reason for the change in catalytic performances of *α*-alkylation, the 5th-recycled poly[St-*co*-AA-*co*-(*R*)-11] was characterized by N_2 adsorption–desorption isotherm, SEM, elemental analysis and IR spectra. It was found that the nitrogen content increased from 0.43% to 0.48%, and the surface area, average pore size and pore volume decreased from 33.5 m^2 g^{-1}, 75.8 nm and 1.27 cm^3 g^{-1} to 6.8 m^2 g^{-1}, 8.4 nm and 0.13 cm^3 g^{-1} respectively, which elucidated that some nitrogen-containing compounds such as *N*-(diphenylmethylene)glycine *tert*-butyl ester and its product were adsorbed in the porous backbone of poly[St-*co*-AA-*co*-(*R*)-11]. Furthermore, the pore size distribution of 5th-recycled poly[St-*co*-AA-*co*-(*R*)-11] showed that the five characteristic diameters of the original micropores at 0.28, 1.26, 1.87, 2.72 and 5.75 nm disappeared and the new pores at 1.77, 2.82, 4.47, 7.47 and 19.02 nm emerged. The same phenomenon was observed for poly[St-*co*-AA-*co*-(*R*)-12] (**Fig.S27**). These enlarged pore diameters were mainly responsible for the enhanced catalytic activity of *α*-alkylation. Due to the enlarged pores in the reused sample, the weakened confinement effect of the enlarged pores on the enantioselectivity was essentially a consequence of subtle change in the transition state induced by the weaker interaction among these pores and reactants. Moreover, the change in the surface morphology of poly[St-*co*-AA-*co*-(*R*)-11] and poly[St-*co*-AA-*co*-(*R*)-12] in the catalytic process was also monitored by SEM. It was observed that more and more particle defects on the surfaces with the prolonging of reaction time within 108 h (**Fig.S28**), which may be the other reason for the enhanced catalytic activity of *α*-alkylation. At the fifth time, no enormous deformation and massive collapse were observed for the SEM image of 5th-recycled poly[St- *co*-AA-*co*-(*R*)-11] (**Fig.S25a**), which stated clearly that poly[St-*co*-AA-*co*-(*R*)-11] possessed the good mechanical stability in the reused process.

4. Conclusions

In this work, the covalent immobilization of simplified Maruoka PTCs onto the framework of polymeric microsphere was developed for the first time to achieve the good reusability of homogeneous simplified Maruoka PTCs. It was of special importance to substantiate that the surface morphology and porous feature of polymer-supported Maruoka PTCs had a significant influence on the catalytic performance including yield and enantioselectivity in the heterogeneous enantioselective α-alkylation. The immobilization of Maruoka PTCs at the 6, 6´-positions of binaphthyl skeleton afforded the superior catalytic results to that of Maruoka PTCs at the close location to quaternary ammonium catalytic site. Moreover, the recovered Maruoka PTCs with good mechanical stability displayed a significantly improved catalytic activity and a little loss in enantioselectivity, which resulted from the improved mass transfer and weakened confinement effect due to the enlarged pores and defects of supported Maruoka PTCs, respectively.

Acknowledgements

We are grateful to the Fundamental Research Funds for the Central Universities [XDJK2015D028] and the National Science Foundation of China [21071116].

Supplementary data

IR, N_2 adsorption–desorption isotherms and SEM of supported PTCs, ^{1}H and ^{13}C NMR and HPLC spectra of products can be found, in the online version, at…...

References

[1] S. Y. Liu, Y. Kumatabara, S. Shirakawa, Green Chem. 18 (2016) 331–341.

[2] S. Shirakawa, K. Maruoka, Angew. Chem. Int. Ed. 52 (2013) 4312–4348.

[3] T. Hashimoto, K. Maruoka, Chem. Rev. 107 (2007) 5656–5682.

[4] B. P. Xiang, K. M. Belyk, R. A. Reamer, N. Yasuda, Angew. Chem. Int. Ed. 53 (2014) 8375–8378.

[5] E. D. F. Martins, J. R. Pliego, ACS Catal. 3 (2013) 613–616.

[6] T. Kano, Y. Hayashi, K. Maruoka, J. Am. Chem. Soc. 135 (2013) 7134–7137.

[7] W. W. Peng, J. W. Wan, B. Xie, X. B. Ma, Org. Biomol. Chem. 12 (2014) 8336–8345.

[8] Y. Liu, S. Shirakawa , K. Maruoka, Org. Lett. 15 (2013) 1230–1233.

[9] B. A. Provencher, K. J. Bartelson, Y. Liu, B. M. Foxman, L. Deng, Angew. Chem. Int. Ed. 50 (2011) 10565–10569.

[10] T. Kano, R. Kobayashi, K. Maruoka, Angew. Chem. Int. Ed. 54 (2015) 8471–8474.

[11] G. R. Humphrey, S. M. Dalby, T. Andreani, B. P. Xiang, M. R. Luzung, Z. J. Song, M. Shevlin, M. Christensen, K. M. Belyk, D. M. Tschaen, Org. Process Res. Dev. 20 (2016) 1097−1103.

[12] S. Shirakawa, K. Ota, S. J. Terao, K. Maruoka, Org. Biomol. Chem. 10 (2012) 5753-5755.

[13] A. Capobianco, A. Di Mola, V. Intintoli, A. Massa, V. Capaccio, L. Roiser, M. Waser, L. Palombi, RSC Adv. 6 (2016) 31861-31870.

[14] A. F. Trindade, P. M. P. Gois, C. A. M. Afonso, Chem. Rev. 109 (2009) 418–514.

[15] W. Wang, X. B. Ma, J. W. Wan, J. Cao, Q. Tang, Dalton Trans. 41 (2012) 5715–5726.

[16] J. Rull, J. J. Jara, R. M. Sebastian, A. Vallribera, C. Najera, J. P. Majoral, A. M. Caminade, ChemCatChem 8 (2016) 2049–2056.

[17] Q. H. Shi, Y.-J. Lee , M.-J. Kim, M.-K. Park , K. Lee, H. R. Song, M. S. Cheng, B.-S. Jeong, H.-g. Park, S.-s. Jew, Tetrahedron Lett. 49 (2008) 1380–1383.

[18] R. Chinchilla, P. Mazón, C. Nájera, Adv. Synth. Catal. 346 (2004) 1186–1194.

[19] S. Itsuno, D. K. Paul, M. Ishimoto, N. Haraguchi, Chem. Lett. 39 (2010) 86–87.

[20] X. Wang, L. Yin, T. Yang, Y. M. Wang, Tetrahedron: Asymmetry 18 (2007) 108–114.

[21] D. D. Feng, J. H. Xu, J. W. Wan, B. Xie, X. B. Ma, Catal. Sci. Technol. 5 (2015) 2141–2148.

[22] S. Itsuno, M. M. Parvez and N. Haraguchi, Poly. Chem. 2 (2011) 1942–1949.

[23] M. Rueping, E. Sugiono, A. Steck, T. Theissmann, Adv. Synth. Catal. 352 (2010) 281–287.

[24] C. Bleschke, J. Schmidt, D. S. Kundu, S. Blechert, A. Thomas, Adv. Synth. Catal. 353 (2011) 3101–3106.

[25] D. S. Kundu, J. Schmidt, C. Bleschke, A. Thomas, S. Blechert, Angew. Chem. Int. Ed. 51 (2012) 5456–5459.

[26] L. Clot-Almenara, C. Rodríguez-Escrich, L. Osorio-Planes, M. A. Pericàs, ACS Catal. 6 (2016) 7647–7651.

[27] S. Shirakawa, Y. Tanaka, K. Maruoka, Org. Lett. 6 (2004) 1429–1431.

[28] Y. Arakawa, N. Haraguchi, S. Itsuno, Angew. Chem. Int. Ed. 47 (2008) 8232–8235.

[29] S. H. Newland, D. J. Xuereb, E. Gianotti, L. Marchese, R. Rios, R. Raja, Catal. Sci. Technol. 5 (2015) 660–665.

[30] T. Wu, D. D. Feng, B. Xie, X. B. Ma, RSC Adv. 6 (2016) 25246–25254.

[31] T. Wu, D. D. Feng, G. X. Xie, X. B. Ma, RSC Adv. 6 (2016) 77396–77405.

[32] L. Lan, G. X. Xie, T. Wu, D. D. Feng, X. B. Ma, RSC Adv. 6 (2016) 55894–55902.

[33] T. Ooi, M. Kameda, K. Maruoka, J. Am. Chem. Soc. 125 (2003) 5139–5151.

[34] M. Kitamura, S. Shirakawa, K. Maruoka, Angew. Chem. Int. Ed. 44 (2005) 1549–1551.

[35] Y. G. Zhang, J. Y. Ying, ACS Catal. 5 (2015) 2681–2691.

Graphical abstract

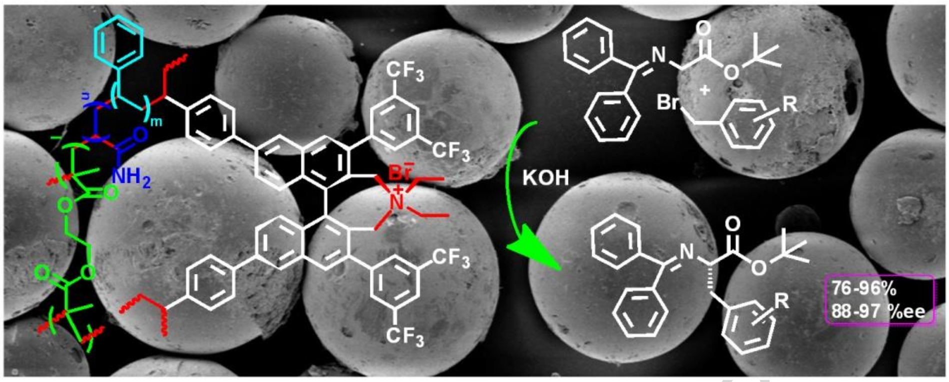

The covalent immobilization of valuable Maruoka catalyst onto poly(styrene-*co*-acrylamide) microsphere was developed for the first time through the copolymerization of styrene-functionalized Maruoka catalyst with styrene and acrylamide by means of suspension polymerization.

Highlights

- The covalent immobilization of Maruoka PTCs onto microsphere for the first time.
- The porous feature of microsphere was responsible for catalytic performance in α-alkylation.
- Good reusability was achieved without significant loss of catalytic performances.